References

BHATTACHARJEE, S., GLUCKSMAN, M. J. & MAKOWSKI, L. (1992). *Biophys. J.* **61**, 725–735.
CHANDRASEKARAN, R., MILLANE, R. P., ARNOTT, S. & ATKINS, E. D. T. (1988). *Carbohydr. Res.* **175**, 1–15.
COCHRAN, W., CRICK, F. H. C. & VAND, V. (1952). *Acta Cryst.* **5**, 581–586.
FRASER, R. D. B., MACRAE, T. P. & MILLER, A. (1964). *Acta Cryst.* **17**, 769–770.
FRASER, R. D. B., MACRAE, T. P. & MILLER, A. (1987). *J. Mol. Biol.* **193**, 115–125.
KAJAVA, A. V. (1991). *J. Mol. Biol.* **218**, 815–823.
KLUG, A., CRICK, F. H. C. & WYCKOFF, H. W. (1958). *Acta Cryst.* **11**, 199–213.
LESLIE, A. G. W., ARNOTT, A., CHANDRASEKARAN, R. & RATLIFF, R. L. (1980). *J. Mol. Biol.* **143**, 49–72.
MAGDOFF-FAIRCHILD, B. & CHIU, C. C. (1979). *Proc. Natl Acad. Sci. USA*, **76**, 223–226.
MAKOWSKI, L. (1982). *J. Appl. Cryst.* **15**, 546–557.
MILLANE, R. P. (1988). *Crystallographic Computing* 4. *Techniques and New Technologies*, edited by N. W. ISAACS & M. R. TAYLOR, pp. 169–186. IUCr/Oxford Univ. Press.
MILLANE, R. P. (1992). *Acta Cryst.* A**48**, 209–215.
MILLANE, R. P., CHANDRASEKARAN, R., ARNOTT, S. & DEA, I. C. M. (1988). *Carbohydr. Res.* **182**, 1–17.
MILLANE, R. P. & STROUD, W. J. (1991). *Int. J. Biol. Macromol.* **13**, 202–208.
NAMBA, K. & STUBBS, G. J. (1985). *Acta Cryst.* A**41**, 252–262.
PAOLETTI, S., CESARO, A. & DELBEN, F. (1983). *Carbohydr. Res.* **123**, 173–178.
PARK, H. S., ARNOTT, A., CHANDRASEKARAN, R., MILLANE, R. P. & CAMPAGNARI, F. (1987). *J. Mol. Biol.* **197**, 513–523.
POTEL, M. J., WELLEMS, T. E., VASSAR, R. J., DEER, B. & JOSEPHS, R. (1984). *J. Mol. Biol.* **177**, 819–839.
REST, M. VAN DER & GARRONE, R. (1991). *FASEB J.* **5**, 2814–2823.
VOTER, W. A., LUCAVECHE, C., BLAUROCK, A. E. & ERICKSON, H. P. (1986). *Biopolymers*, **25**, 2359–2373.

Acta Cryst. (1995). A**51**, 365–374

Orientational Order and Disorder in Solid C_{60}: Theory and Diffraction Experiments

BY K. H. MICHEL

Department of Physics, Universiteit Antwerpen (UIA), 2610 Wilrijk, Belgium

D. LAMOEN

Max-Planck-Institut für Festkörperforschung, Postfach 800665, 70506 Stuttgart, Germany

AND W. I. F. DAVID

ISIS Science Division, Rutherford Appleton Laboratory, Chilton, Didcot, Oxon OX11 0QX, England

(*Received* 20 *July* 1994; *accepted* 16 *November* 1994)

Abstract

Starting from a microscope model of the intermolecular potential, a unified description is presented of the Bragg scattering law in the orientationally disordered and in the ordered phase of solid C_{60}. The orientational structure factor is expanded in terms of symmetry-adapted surface harmonics. The expansion coefficients are calculated from theory and compared with experiment. Their temperature evolution is studied in the disordered phase at the 260 K transitions and in the ordered phase. In the ordered phase, new results from high-resolution neutron powder diffraction are given. In the disordered phase, space group $Fm\bar{3}m$, the reflections have A_{1g} symmetry; in the ordered phase, space group $Pa\bar{3}$, reflections of T_{2g} symmetry appear and in addition the A_{1g} reflections are renormalized. The orientational density distribution is calculated. The effective crystal-field potential is constructed, its temperature evolution in the ordered phase is studied and related to the occurrence of an orientational glass.

1. Introduction

C_{60}-fullerite is a molecular crystal (Krätschmer, Lamb, Fostiropoulos & Huffman, 1990). At room temperature, the space group is $Fm\bar{3}m$ (Fleming *et al.*, 1991) and the molecules are orientationally disordered. At a transition temperature $T_1 \simeq 260$ K, the crystal undergoes a phase change (Dworkin *et al.*, 1991; Heiney *et al.*, 1991*a*) to a $Pa\bar{3}$ structure (Sachidanandam & Harris, 1991; Heiney *et al.*, 1991*b*; David *et al.*, 1991). The molecules are orientationally ordered on four different sublattices (Harris & Sachidanandam, 1992). Neutron powder diffraction (David *et al.*, 1991) and single-crystal X-ray studies (Liu, Lu, Kappes & Ibers, 1991; Bürgi *et al.*, 1992) of the low-temperature ordered structure have revealed the packing configuration of the C_{60} molecules. In an optimized ordering scheme, electron-rich double bonds that fuse the hexagons on the C_{60} molecule face pentagons of adjacent C_{60} units. This idea has been implemented in molecular dynamics calculations (Sprik, Cheng & Klein, 1992). A theoretical description of the

orientationally disordered phase and the phase transition has been formulated with the use of multipolar rotator functions (Michel, Copley & Neumann, 1992); for a review we refer to Axe, Moss & Neumann (1994).

In the disordered phase, the molecules are not free rotators but experience a crystal field of cubic symmetry, as was first suggested by theory. The Bragg reflections have A_{1g} symmetry. X-ray synchrotron diffraction experiments on single crystals (Chow *et al.*, 1992), high-resolution neutron powder diffraction (David, Ibberson & Matsuo, 1993) and single-crystal neutron diffraction (Papoular, Roth, Heger, Haluska & Kuzmany, 1993) experiments have allowed the determination of the orientational density distribution function in the disordered phase. The orientational density distribution function is related to the crystal field (Press & Hüller, 1973*a*), and since the crystal field depends on the molecular structure, the diffraction experiments allow the testing of theoretical models of intermolecular potentials (Copley & Michel, 1993). The interpretation of diffraction experiments has revealed that the single-molecule orientational distribution function in the disordered phase exhibits maxima (Lamoen & Michel, 1993*a*; Bürgi, Restori & Schwarzenbach, 1993; Axe, Moss & Neumann, 1994) for the same orientations that correspond to the setting angles (majority positions) of the molecules on the four sublattices in the fully ordered $Pa\bar{3}$ stucture (David *et al.*, 1991; David, Ibberson, Dennis, Hare & Prassides, 1992; Bürgi *et al.*, 1992). These results show that local orientational order in the high-temperature phase, which is a consequence of the crystal field, also affects the collective ordering in the low-temperature phase. In the present paper, our aim is the understanding of the orientational density distribution function in the disordered and in the ordered phase from a unified point of view. Also in the ordered phase, as we will see in the following, high-resolution neutron powder diffraction experiments allow the determination of the orientational density distribution function.

The content of the paper is as follows. In §2, we recall basic concepts of our theoretical description of solid C_{60}. In §3, we recall the Bragg scattering law for the disordered phase and we derive the scattering law for the ordered phase. These scattering laws are formulated in terms of multipole expansions by means of symmetry-adapted surface harmonics. The expansion coefficients (also called diffraction coefficients) are calculated by use of statistical mechanics in §4. In the disordered phase, the Bragg reflections have A_{1g} symmetry and are slightly temperature dependent. In the ordered phase, additional reflections of T_{2g} symmetry appear and, furthermore, an important renormalization of the A_{1g} reflections occurs. We present high-resolution neutron powder diffraction data on the A_{1g} reflections in the ordered phase. The remarkable temperature dependence of these reflections is explained by theory. The influence of the lattice contraction is investigated. The orientational density distribution is calculated. In §5, we derive an effective temperature-dependent crystal field potential and study the freezing of orientational motion.

2. Model of molecular crystal C_{60}

Here, we briefly recall some basic concepts that have been introduced previously for a description of solid C_{60} (Michel, Copley & Neumann, 1992; Michel, 1992). We consider a crystal that consists of N rigid molecules of C_{60} with centres of mass rigidly located at f.c.c. lattice sites $\mathbf{X}(\mathbf{n})$. Molecules may rotate about their centres of mass. Each molecule is represented by 60 atomic centres, 60 single-bond centres and a distribution of three centres alng each of the 30 double bonds. Centres are labelled ν_A, where $A = a, b$ or s denotes atoms, double bonds or single bonds, respectively. The position of the centre ν_A belonging to the molecule at lattice site $\mathbf{n}$ is written

$$\mathbf{X}(\mathbf{n}, \nu_A) = \mathbf{X}(\mathbf{n}) + \mathbf{d}(\mathbf{n}, \nu_A), \tag{2.1}$$

where the direction of the vector $\mathbf{d}(\mathbf{n}, \nu_A)$ is described by two polar angles $\Omega(\nu_A) = [\theta(\nu_A), \varphi(\nu_A)]$. All centres are located on a spherical shell with radius d. The potential between two molecules is determined by the sum of interactions between their centres. Orientation-dependent properties of molecules in crystals can be described by means of rotator functions (James & Keenan, 1959; Press & Hüller, 1973*b*). They are defined by symmetry-adapted linear combinations (Yvinec & Pick, 1980; Michel & Parlinski, 1985) of Wigner's rotation matrices D_l^{nm}

$$U_l^{1\tau}(\omega) = \sum_{nm} \alpha_{l(M)}^{n1} D_l^{nm}(\omega) \alpha_{l(S)}^{m\tau}. \tag{2.2}$$

Here, ω are the Euler angles, which describe the orientation of the molecule, l is the angular momentum quantum number. The coefficients $\alpha_{l(M)}^{n1}$ refer to the symmetry of the molecule. Icosahedral symmetry of the C_{60} molecule (Kroto, Heath, O'Brien, Curl & Smalley, 1985) restricts the values of l to 0, 6, 10, 12, ... The coefficients $\alpha_{l(s)}^{m\tau}$ account for the symmetry of the site, $S = O_h$. The index τ stands for (Γ, ρ, i). Here Γ labels the irreducible representations of the cubic group, ρ distinguishes between representations that occur more than once and i denotes the row of a given representation.

Expanding the intermolecular potential in terms of rotator functions and summing over all pairs of molecules in the lattice, we obtain the lattice potential $V = V^{RR} + V_{CF}$. Here, V^{RR} is the rotation–rotation (RR) interaction:

$$V^{RR} = (1/2) \sum_{\mathbf{nn}} \sum_{ll'} \sum_{\tau\tau'} J_{ll'}^{\tau\tau'}(\mathbf{n} - \mathbf{n}') U_l^{1\tau}(\mathbf{n}) U_{l'}^{1\tau'}(\mathbf{n}'); \tag{2.3}$$

the argument $\mathbf{n}$ of $U_l^{1\tau}(\mathbf{n})$ stands for $\omega(\mathbf{n})$. V_{CF} represents

Table 1. *Crystal field coefficients* $w_l^{(\rho)}$ *for disordered phase* (I) *and ordered phase* (II) *from Lamoen & Michel* (1994)

l, ρ	$w_l^{(\rho)}$ (I) (K)	$w_l^{(\rho)}$ (II) (K)
6,1	470.34	383.94
10,1	−172.18	−194.48
12,1	−77.31	−90.51
12,2	−347.89	−412.46

the crystal field,

$$V_{\mathrm{CF}} = \sum_{\mathbf{n}} \sum_{l} \sum_{\tau_{1g}} w_l^{\tau_{1g}} U_l^{1\tau_{1g}}(\mathbf{n}), \tag{2.4}$$

where $\tau_{1g} = (A_{1g}, \rho)$. V_{CF} has full cubic symmetry and the index ρ labels the A_{1g} representations for a given l. For $l = 6$ and 10, $\rho = 1$, while, for $l = 12$, $\rho = 1$ or 2. In the following, we write $w_l^{(\rho)}$ for $w_l^{\tau_{1g}}$. The expansion coefficients $J_{ll'}^{\tau\tau'}$ and $w_l^{\tau_{1g}}$ are determined by numerical calculations. In Table 1, we have quoted the crystal-field coefficients $w_l^{(\rho)}$ for two different values of the cubic lattice constant a, taking 14.15 Å for the disordered phase and 14.10 Å for the ordered phase. These results will be used in §4.

It is convenient to introduce Fourier transforms

$$U_l^{1\tau}(\mathbf{k}) = (1/N^{1/2}) \sum_{\mathbf{n}} U_l^{1\tau}(\mathbf{n}) \exp[-i\,\mathbf{k} \cdot \mathbf{X}(\mathbf{n})], \tag{2.5}$$

where $\mathbf{k}$ is the wave vector. It has been shown previously (Michel, Copley & Neumann, 1992) that the phase transition from the orientationally disordered phase with space group $Fm\bar{3}m$ to the orientationally ordered $Pa\bar{3}$ phase is driven by the condensation of orientational modes with symmetry $\tau = (T_{2g}, \rho, i)$ at the X point of the Brillouin zone. In the following, we will restrict ourselves to the mode T_{2g}, $\rho = 3$ of the manifold $l = 10$, which we consider as the leading mode, and to the mode T_{2g}, $\rho = 2$ for $l = 6$. We will abbreviate the notation by writing U_l^i for $U_l^{1\tau}$. The index i refers to the three components of T_{2g} symmetry. We write $J_{ll'}^{ij}$ for the interaction coefficients of these modes: the symmetry reduction at the phase transition is represented by

$$\begin{aligned} Fm\bar{3}m\colon [\mathbf{k}^X, U_l^{3e}(\mathbf{k}_x^X) &= U_l^{2e}(\mathbf{k}_z^X) = U_l^{1e}(\mathbf{k}_y^X) \\ &= N^{1/2}\eta_l \neq 0; \\ U_l^{2e}(\mathbf{k}_x^X) &= U_l^{3e}(\mathbf{k}_y^X) \\ &= U_l^{1e}(\mathbf{k}_z^X) = 0] \rightarrow Pa\bar{3}. \end{aligned} \tag{2.6}$$

Here the index e indicates that U_l^{ie} is a thermal expectation value; the star of wave vectors of the condensing modes is $\mathbf{k}_x^X = (2\pi/a, 0, 0)$, $\mathbf{k}_y^X = (0, 2\pi/a, 0)$, $\mathbf{k}_z^X = (0, 0, 2\pi/a)$, where a is the cubic lattice constant. In real space, the condensation scheme corresponds to the distribution of the order-parameter components (η_l, η_l, η_l); $(-\eta_l, -\eta_l, \eta_l)$; $(\eta_l, -\eta_l, -\eta_l)$; $(-\eta_l, \eta_l, -\eta_l)$ on the sublattices (0, 0, 0); $a/2$ (0, 1, 1); $a/2$ (1, 0, 1) and $a/2$ (1, 1, 0), respectively. Labelling the sublattices by $\sigma = 0, 1, 2$ and 3, respectively, we introduce the vectors $\eta_l(\sigma)$ with components $\eta_l^i(\sigma)$, $i = 1, 2, 3$. At the X point of the Brillouin zone, the Fourier-transformed interaction $J_{ll'}^{ij}(\mathbf{k})$ becomes attractive and has a maximum:

$$J_{ll'}^{ij}(\mathbf{k}_\alpha^X) = -J_{ll'}\delta_{ij}, \tag{2.7}$$

where, for $\alpha = x$, i has values 2 or 3, for $\alpha = y$, $i = 1, 3$ and for $\alpha = z$, $i = 1, 2$. Taking as value of the lattice constant $a = 14.10$ Å, Lamoen & Michel (1994) have obtained $J_{10\,10} = 4693.5$, $J_{6\,6} = 1950.1$, $J_{6\,10} = 321.2$ K. The large value of $J_{10\,10}$ has led to the conclusion that the phase transition is primarily driven by the condensation of the dominant mode T_{2g}, $\rho = 3$ belonging to the manifold $l = 10$.

In the molecular-field approximation, the interaction V^{RR} reads

$$V_{\mathrm{MF}}^{RR} = -\sum_{ll'} \sum_{\sigma} \sum_{\mathbf{n}_\sigma} \sum_{i} J_{ll'}\, U_l^i(\mathbf{n}_\sigma)\eta_{l'}^i(\sigma). \tag{2.8}$$

Here $\mathbf{n}_\sigma$ runs over all sites of the sublattic σ. The total lattice potential now becomes

$$V_{\mathrm{MF}} = V_{\mathrm{MF}}^{RR} + V_{\mathrm{CF}}. \tag{2.9}$$

The order-parameter components are then given by

$$\eta_l^i(\sigma) = \langle U_l^i(\mathbf{n}_\sigma)\rangle_{\mathrm{MF}} = \frac{\mathrm{Tr}[U_l^i(\mathbf{n}_\sigma)\exp(-V_{\mathrm{MF}}/T)]}{\mathrm{Tr}[\exp(-V_{\mathrm{MF}}/T)]}. \tag{2.10}$$

Here, the trace Tr stands for an integration over Euler angles. In a previous work (Lamoen & Michel, 1994), the order-parameter amplitude η_{10} was obtained from a Landau expansion of the free energy. A first-order phase transition occurs at a temperature $T_1 = 201.9$ K. The temperature evolution of η_{10} is given in the last column of Table 3, §4. Owing to the coupling $J_{6\,10}$, a condensation of η_{10}^i entails a condensation of η_6^i. In linear approximation we find for the amplitude

$$\eta_6 = J_{6\,10}/T\langle(U_6^j)^2\rangle_{\mathrm{CF}}\eta_{10}, \tag{2.11}$$

where the thermal average is calculated with V_{CF}. At the transition we obtain $\eta_{10} \simeq -0.067$ and $\eta_6 \simeq -0.01$. The values of η_{10} quoted in Table 3 have been calculated under the assumption $\eta_6 = 0$, that is $J_{6\,10} \simeq 0$.

3. Bragg scattering law

We will consider the differential scattering cross section for neutrons and X-rays (synchrotron radiation). The results obtained for the case of neutron scattering will also apply to X-ray scattering (Copley & Michel, 1993). This point of view is cofirmed by combined neutron and X-ray diffraction experiments on single crystals of C_{60} (Papoular, Roth, Heger, Haluska & Kuzmany, 1993).

Table 2. *Molecular shape factor*

l	0	6	10	12
g_l^a	16.92	2.56	19.35	7.89

The Bragg part of the total differential scattering cross section per unit solid angle Ω_Q reads

$$d\sigma/d\Omega_Q|_B = \left| \sum_{\mathbf{n}} \exp[i\mathbf{Q}\cdot\mathbf{X}(\mathbf{n})]\langle F_{\mathbf{n}}^a(\mathbf{Q})\rangle \right|^2 \lambda_C^2. \quad (3.1)$$

Here $\hbar\mathbf{Q}$ is the momentum transferred in the scattering process, λ_C is the neutron scattering length for the carbon nucleus, and $F_{\mathbf{n}}^a(\mathbf{Q})$ is the molecular structure factor

$$F_{\mathbf{n}}^a(\mathbf{Q}) = \sum_{\nu_a} \exp[i\mathbf{Q}\cdot\mathbf{d}(\mathbf{n}, \nu_a)]. \quad (3.2)$$

Expanding in terms of molecular rotator functions (Press & Hüller, 1973*a*; Pick & Yvinec, 1980), we obtain

$$F_{\mathbf{n}}^a(\mathbf{Q}) = 4\pi \sum_l \sum_\tau j_l(Qd)\, i^l\, g_l^a S_l^\tau(\Omega_\mathbf{Q}) U_l^{1\tau}(\mathbf{n}). \quad (3.3)$$

Here, j_l denotes the Bessel function. The quantity g_l^a defines the molecular shape factor [originally called the form factor (Michel & Parlinski, 1985)] due to the configuration of atomic nuclei. Numerical values of g_l^a are given in Table 2. The functions S_l^τ are the site-symmetry-adapted surface harmonics (Bradley & Cracknell, 1972).

(*a*) *Disordered phase*

This case has been studied previously (Copley & Michel, 1993) and we only recall the main result. At any site of the f.c.c. lattice, the time-averaged symmetry is A_{1g}. One obtains for the Bragg scattering cross section

$$d\sigma/d\Omega_\mathbf{Q}|_B = [N(2\pi)^3/V_C] \sum_\mathbf{G} \delta(\mathbf{Q}-\mathbf{G}) |4\pi \times \sum_l \sum_\rho j_l(Qd) i^l K_l^{(\rho)}(\Omega_\mathbf{Q}) \gamma_l^{(\rho)}|^2 \lambda_C^2. \quad (3.4)$$

Here, $V_C = a^3/4$ is the volume of the primitive unit cell of the f.c.c. lattice, $\mathbf{G}$ is a reciprocal-lattice vector. We have used the cubic harmonics (Bethe, 1929)

$$K_l^{(\rho)}(\Omega) \equiv S_l^{\tau_{1g}}(\Omega), \quad \tau_{1g} = (A_{1g}, \rho). \quad (3.5)$$

The thermal coefficients

$$\gamma_l^{(\rho)} = g_l^a \langle U_l^{1\tau_{1g}}\rangle_{CF} \quad (3.6)$$

are calculated with use of the crystal field.

(*b*) *Ordered phase*

The orientational order breaks the translation symmetry of the orientation density on the four sublattices. Distinguishing between the sublattices, we write for the Bragg scattering cross section

$$d\sigma/d\Omega_\mathbf{Q}|_B = \left| \sum_\sigma \sum_{\mathbf{n}_\sigma} \exp[i\mathbf{Q}\cdot\mathbf{X}(\mathbf{n}_\sigma)] \langle F_{\mathbf{n}_\sigma}^a(\mathbf{Q})\rangle \right|^2 \lambda_C^2, \quad (3.7)$$

where $F_{\mathbf{n}}^a$ is given by expression (3.3) with $\mathbf{n}$ replaced by $\mathbf{n}_\sigma$. In calculating the thermal average, we take into account the molecular field potential (2.9) and retain only contributions of A_{1g} and T_{2g} symmetry. The $Pa\bar{3}$ space group permits the occurence of non-zero thermal averages of A_{2g} and T_{1g} symmetry (see *e.g.* Heid, 1993; Rapcewicz & Przystawa, 1994). Their effect is to rotate the C_{60} molecular orientation away from the (110) mirror planes of $Fm\bar{3}m$. Experimental evidence shows that this deviation is very small (Bürgi *et al.*, 1992). In the following, we will neglect contributions of A_{2g} and T_{1g} symmetry. The thermally averaged molecular structure factor now reads

$$\langle F_{\mathbf{n}_\sigma}^a(\mathbf{Q})\rangle_{MF} = \langle F^{a,A_{1g}}(\mathbf{Q})\rangle_{MF} + \langle F_\sigma^{a,T_{2g}}(\mathbf{Q})\rangle_{MF}, \quad (3.8)$$

where

$$\langle F^{a,A_{1g}}(\mathbf{Q})\rangle_{MF} = 4\pi \sum_l \sum_\rho j_l(Qd)\, i^l K_l^{(\rho)}(\Omega_\mathbf{Q}) \gamma_l^{(\rho)} \quad (3.9)$$

and

$$\langle F_\sigma^{a,T_{2g}}(\mathbf{Q})\rangle_{MF} = -4\pi \sum_l \sum_{i=1}^{3} j_l(Qd) S_l^i(\Omega_\mathbf{Q})\, g_l^a\, \eta_l^i(\sigma). \quad (3.10)$$

In expression (3.9), we have defined

$$\gamma_l^{(\rho)} = g_l^a \langle U_l^{1\tau_{1g}}\rangle_{MF}. \quad (3.11)$$

With the use of (3.8)–(3.10), we rewrite the scattering cross section within $Fm\bar{3}m$ as

$$d\sigma/d\Omega_\mathbf{Q}|_B = d\sigma/d\Omega_\mathbf{Q}|_B^{A_{1g}} + d\sigma/d\Omega_\mathbf{Q}|_B^{T_{2g}}. \quad (3.12)$$

Here, the first term on the right-hand side has the same form as (3.4); however, $\gamma_l^{(\rho)}$ is given by (3.11) instead of (3.6). As we will show in §4, this fact leads to an important renormalization of the reflections of A_{1g} symmetry in the ordered phase. The second term reads.

$$d\sigma/d\Omega_\mathbf{Q}|_B^{T_{2g}} = (N_1/V_1)(2\pi)^3 \sum_{l,l'} \sum_{G^x} \delta(\mathbf{Q}-\mathbf{G}^x)(4\pi)^2 \times \left\{ j_l(Qd) g_l^a\, j_{l'}(QD) g_{l'}^a \left[\sum_\sigma I_{ll'}^{\sigma\sigma}(\mathbf{Q}) + \sum_{\sigma\sigma'}{}' I_{ll'}^{\sigma\sigma}(\mathbf{Q}) \cos(\mathbf{Q}\cdot\mathbf{r}^{\sigma\sigma'}) \right] \right\} \lambda_C^2, \quad (3.13)$$

where the prime on the summation sign indicates $\sigma \neq \sigma'$

and where

$$I_{ll'}^{\sigma\sigma'}(\mathbf{Q}) = \left[\sum_{i=1}^{3} \eta_l^i(\sigma) S_l^i(\Omega_\mathbf{Q})\right]\left[\sum_{j=1}^{3} \eta_{l'}^j(\sigma') S_{l'}^j(\Omega_\mathbf{Q})\right]. \tag{3.14}$$

In (3.13), we have $N_1 = N/4$, $V_1 = a^3$ and $\mathbf{G}^X$ is a reciprocal-lattice vector of the simple cubic lattice with lattice constant a. The vector $\mathbf{r}^{\sigma\sigma'}$ relates neighbouring molecules with different orientations. In deriving (3.12), we have verified that there are no interference terms between contributions from A_{1g} and T_{2g} symmetry. In the following section, we will show how the scattering law is related to the orientational density distribution function.

The orientational ordering in solid C_{60} has been investigated in an important paper by Harris & Sachidanandam (1992). Starting from the positions of oriented icosahedra on a f.c.c. lattice for the space group $Pa\bar{3}$, these authors have derived symmetry relations between the structure factors of the four molecules in the unit cell of the simple cubic lattice. For instance, the structure factor of the molecule centred at (0,0,0) (labelled by the subscript 0) is related to the structure factor of the molecule centred at $(0, a/2, a/2)$ (labelled by subscript 1) by

$$F_0(Q_x, Q_y, Q_z) = F_1(Q_x, Q_y, -Q_z). \tag{3.15}$$

Similar relations are obtained for the other pairs of molecules in the simple cubic unit cell.

We will now show that our formulation of the structure factor in terms of symmetry-adapted surface harmonics is in agreement with relation (3.15). Using the structure factor (3.10), we get for the molecule centred at (0,0,0)

$$\langle F_0^{a,T_{2g}}(\mathbf{Q})\rangle = \sum_l C_l(Q)[S_l^1(\Omega_\mathbf{Q}) + S_l^2(\Omega_\mathbf{Q}) + S_l^3(\Omega_\mathbf{Q})]\eta_l, \tag{3.16}$$

and for the molecule centred at $(0, a/2, a/2)$

$$\langle F_1^{a,T_{2g}}(\mathbf{Q})\rangle = \sum_l C_l(Q)[-S_l^1(\Omega_\mathbf{Q}) - S_l^2(\Omega_\mathbf{Q}) + S_l^3(\Omega_\mathbf{Q})]\eta_l, \tag{3.17}$$

where $C_l = 4\pi j_l(Qd) g_l^a$. We observe that the surface harmonics $S_l^i(\Omega_\mathbf{Q})$ of T_{2g} symmetry transform as $\hat{Q}_y\hat{Q}_z$, $\hat{Q}_z\hat{Q}_x$ and $\hat{Q}_x\hat{Q}_y$ for $i = 1, 2$ and 3, respectively, where $\hat{Q}_x = Q_x/Q$, $\hat{Q}_y = Q_y/Q$, $\hat{Q}_z = Q_z/Q$. It is now obvious that (3.16) and (3.17) are related by an equation similar to (3.15). It is straightforward to show that the contributions (3.9) to the structure factor also satisfy the same symmetry relations. Indeed, the cubic harmonics of A_{1g} symmetry are even functions of $\hat{Q}_x$, $\hat{Q}_y$ and $\hat{Q}_z$. We conclude that the present structure factors fulfil the general symmetry relations of the $Pa\bar{3}$ structure that were derived by Harris & Sachidanandam (1992). This result is important; it demonstrates the validity of our formulation of the $Pa\bar{3}$ structure in terms of surface harmonics of A_{1g} and T_{2g} symmetry.

4. Diffraction coefficients and orientational distribution

Here, we will investigate the diffraction coefficients that refer to the reflections of A_{1g} symmetry. In the disordered phase, they are calculated by using (3.6), the thermal average being taken with the crystal field V_{CF}. In the ordered phase, we use (3.11) with the mean field potential V_{MF}. The calculations have been performed by taking the values of the crystal-field coefficients $w_l^{(\rho)}$ from Table 1. The results obtained by numerical integrations are quoted in Table 3 for a series of temperatures. We have restricted ourselves here to values of $l \leq 12$. Notice the change of sign of $\gamma_6^{(1)}$ in the ordered phase.

We have seen in §3 that the coefficients $\gamma_l^{(\rho)}$ can be determined from diffraction experiments. For the case of the disordered phase, a synchrotron X-ray study on single crystals was carried out at room temperature by Chow *et al.* (1992). More recently, neutron powder diffraction (NPD) data became available (David, Ibberson & Matsuo, 1993). The coefficients $C_{l\rho}$ obtained in the work of Chow *et al.* are related to the coefficients $\gamma_l^{(\rho)}$ in the present paper by $\gamma_l^{(\rho)} = g_0^a C_{l\rho} \times 10^{-3}$, where $g_0^a = 60/(4\pi)^{1/2}$. We have quoted the corresponding quantities $\gamma_l^{(\rho)}$ in Table 4. In taking over the neutron powder diffraction results from experiment, we should mention that, owing to a normalization error, the coefficients $C_{l\rho}$ for $l \neq 0$ quoted by David, Ibberson & Matsuo (1993) are too large by a factor of $2^{1/2}$. After correcting this error, we have obtained the values NPD in Table 4. In comparing the experimental data with the theoretical values of the coefficients $\gamma_l^{(\rho)}$ for $T > T_1$ from Table 3, we see that the signs of all coefficients for $l \leq 12$ are correct and that the numerical values are, in general, fair. A discrepancy remains: the theoretical value of $\gamma_{10}^{(1)}$ because the absolute value of the crystal-field coefficient $w_{10}^{(1)}$ is too large. We will come back to this point in §5.

High-resolution neutron powder diffraction measurements of the coefficients $\gamma_l^{(\rho)}$ have been extended by one of the authors (WIFD) to the ordered phase. The results are shown in Fig. 1. Most remarkable is the temperature behaviour of $\gamma_6^{(1)}$, which changes sign near T_1. In comparing these results with the theoretical calculations of $\gamma_l^{(\rho)}$ in Table 3, we see that the overall temperature dependence is described fairly well by theory. Our theoretical results become less valid at lower T since our method of calculating the order-parameter amplitude by means of a Landau expansion of the energy becomes unreliable.

It is instructive to have analytical expressions for the diffraction coefficients by performing high-temperature

Table 3. *Calculated values of diffraction coefficients* $\gamma_l^{(\rho)}$ *and of order-parameter amplitude* η_{10}

$T_1 = 201.9$ K is the calculated transition temperature.

T	$\gamma_6^{(1)}$	$\gamma_{10}^{(1)}$	$\gamma_{12}^{(1)}$	$\gamma_{12}^{(2)}$	η_{10}
1.238 T_1	−0.430	0.840	0.038	0.599	0
1.015 T_1	−0.525	1.051	0.036	0.766	0
T_1	−0.444	0.894	0.135	0.924	−0.067
0.941 T_1	−0.373	0.970	0.278	1.283	−0.154
0.867 T_1	−0.247	1.252	0.510	1.766	−0.214
0.792 T_1	−0.037	1.963	0.810	2.201	−0.266
0.743 T_1	0.1639	2.774	1.041	2.412	−0.300

Table 4. *Experimental diffraction coefficients at room temperature*

X: synchrotron X-rays; NPD: neutron powder diffraction. Compare with values at $1.238T_1$ in Table 3.

	$\gamma_6^{(1)}$	$\gamma_{10}^{(1)}$	$\gamma_{12}^{(1)}$	$\gamma_{12}^{(2)}$
X	−0.386	0.217	0.159	0.440
NPD	−0.395	0.359	0.228	0.0706

series expansions. Starting from expression (3.6), one obtains in the disordered phase (Lamoen & Michel, 1993*a*) for the coefficients of A_{1g} modes

$$\gamma_l^{(\rho)} \simeq -g_l^a w_l^{(\rho)}/[T(2l+1)]. \quad (4.1)$$

Taking the molecular shape factors from Table 2 and the crystal-field coefficients from column I of Table 1, we find that the approximate values agree in sign and in order of magnitude with the numerical results of Table 3.

We now turn to a discussion of the coefficients $\gamma_l^{(\rho)}$ of A_{1g} modes in the ordered phase near T_1, starting from (3.11). At the first-order phase transition, the order-parameter amplitude changes discontinuously from zero to a finite (negative) value. In addition, this change induces a discontinuous lattice contraction. Both effects modify the potential V_{MF}, equation (2.9). The first one leads to the interaction $V_{MF}{}^{RR}$, equation (2.8), the second one changes the crystal-field coefficients $w_l^{(\rho)}$ (see Table 1). Consequently, we write for $\gamma_l^{(\rho)}$ at the transition and in the ordered phase

$$\gamma_l^{(\rho)} = \gamma_l^{(\rho)}|_{CF} + \Delta\gamma_l^{(\rho)}|_{RR} + \Delta\gamma_l^{(\rho)}|_{latt}. \quad (4.2)$$

The term due to lattice contraction can be approximated by using (4.1) as

$$\Delta\gamma_l^{(\rho)}|_{latt} = -g_l^a[w_l^{(\rho)}(II) - w_l^{(\rho)}(I)]/[T(2l+1)], \quad (4.3)$$

where $w_l^{(\rho)}(II)$ and $w_l^{(\rho)}(I)$ refer to the values of the crystal-field coefficients in the ordered and in the disordered phase, respectively. Using the values of Table 1, we see that (4.3) leads to positive contributions to $\gamma_l^{(\rho)}$ at the transition from the disordered to the ordered phase. It is instructive to relate $\Delta\gamma_l^{(\rho)}|_{latt}$ to the orientational order parameter. We observed that the change of the crystal-field coefficients depends on the lattice contraction Δa. In first order, we write

$$w_l^{(\rho)}(II) - w_l^{(\rho)}(I) = G_l^{(\rho)}\Delta a. \quad (4.4)$$

Since $\Delta a < 0$, we deduce that the coefficients $G_l^{(\rho)}$ are positive. The lattice contraction is related to the change of the order parameter (Lamoen & Michel, 1993*b*):

$$\Delta a = -8a^{-1}|\Lambda|\kappa_L \eta_{10}^2, \quad (4.5)$$

where Λ is a microscopic coupling coefficient and where κ_L is the compressibility. Substituting the last two relations into (4.6), we get

$$\Delta\gamma_l^{(\rho)}|_{latt} = [8g_l^a G_l^{(\rho)}|\Lambda|\kappa_L/aT(2l+1)]\eta_{10}^2. \quad (4.6)$$

This contribution is positive and increases in the ordered phase. The remaining terms on the right-hand side of (4.2) are obtained by performing a series expansion in terms of η_{10} in (3.11) and by retaining the crystal field of the uncontracted lattice. We then find that the zeroth-order term $\gamma_l^{(\rho)}|_{CF}$ is given by (3.6) while the contribution from the order parameter reads

$$\Delta\gamma_l^{(\rho)}|_{RR} = [3g_l^a J_{10\,10}^2 q_l^{(\rho)}/2T^2 Z_{CF}]\eta_{10}^2. \quad (4.7)$$

Here the factor Z_{CF} corresponds to the denominator of (2.10) with V_{MF} replaced by V_{CF}. The coefficients $q_l^{(\rho)}$ are defined by

$$q_l^{(\rho)} = \int d\omega\, U_l^{1\tau_{1g}}(\omega)[U_{10}^j(\omega)]^2, \quad (4.8)$$

where $\tau_{1g} = (A_{1g}, \rho)$. Since the square of a T_{2g} mode has symmetry A_{1g}, the coefficients $q_l^{(\rho)}$ are non-zero. This fact accounts for the renormalization of the diffraction coefficients $\gamma_l^{(\rho)}$ by the condensation of an order parameter of different symmetry (*in casu* T_{2g} *versus* A_{1g}). By numerial integrations we find $q_6^{(1)} = 0.1834$, $q_{10}^{(1)} = 0.0379$, $q_{12}^{(1)} = -0.0142$, $q_{12}^{(2)} = 0.0075$.

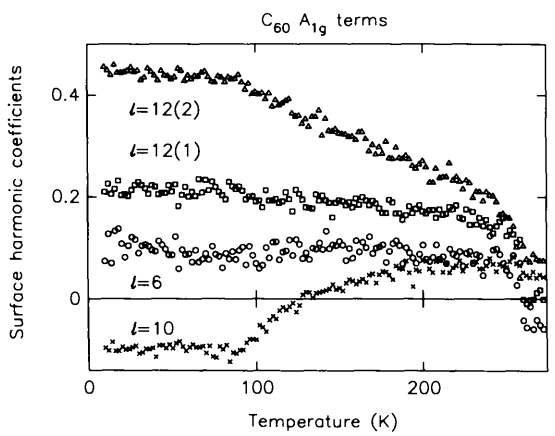

Fig. 1. Temperature evolution of coefficients $\gamma_l^{(\rho)}$ obtained from high-resolution neutron powder diffraction.

We will now discuss in more detail the temperature behaviour of $\gamma_6^{(1)}$ by returning to (4.2). The contribution $\gamma_6^{(1)}|_{CF}$ is always negative, since $w_6^{(1)} > 0$. On the other hand, the contributions $\Delta\gamma_6^{(\rho)}|_{RR}$ and $\Delta\gamma_6^{(\rho)}|_{latt}$ are positive and increase quadratically with η_{10} in the ordered phase. It is therefore conceivable that $\gamma_6^{(1)}$ becomes positive in the ordered phase. In Fig. 2, we have plotted the temperature evolution of $\gamma_6^{(1)}$, obtained by numerical integrations from (3.6) and (3.11). We see that $\gamma_6^{(1)}$ changes sign near 0.79 T_1. In experiment (see Fig. 1), the change of sign occurs closer to T_1. This discrepancy is due to the fact that our theoretical value of η_{10} is too low, which in turn can be traced back to the fact that our positive value of $w_6^{(1)}$ is too large (see discussion in the next section). Experimentally, one finds that the first-order charcter of the phase transition is rather pronounced (David *et al.*, 1992; Heiney *et al.*, 1992; Moret *et al.*, 1992). We have verified that an order parameter of symmetry T_{2g} belonging to the second representation of the manifold $l = 6$ does not cause a change of sign of $\gamma_6^{(1)}$. In other words, the remarkable temperature behaviour of $\gamma_6^{(1)}$ provides direct experimental support for an orientational order parameter belonging to the manifold $l = 10$, as was suggested by Michel, Copley & Neumann (1992). The relative importance of multipoles with $l = 10$ is also supported by quasi-elastic neutron scattering results (Neumann *et al.*, 1991). More recently, Yildirim, Harris, Erwin & Pederson (1993) have demonstrated the importance of multipoles belonging to the manifold $l = 10$ by *ab initio* calculations of the electronic charge density of the C_{60} molecule. Finally, we have investigated the influence of the sign of η_{10} on $\gamma_6^{(1)}$ by studying the correction of order $(\eta_{10})^3$. We obtain a positive contribution to $\gamma_6^{(1)}$ under the condition that $\eta_{10} < 0$. Since experiments show that $\gamma_6^{(1)}$ remains positive at low T, we have additional evidence for the negative value of η_{10}.

We now turn to the evaluation of the orientational density distribution function. We start from the instantaneous orientational density distribution for nuclei of a molecule at lattice site **n**, which we write (Michel & Parlinski, 1985) as

$$f(\Omega; \mathbf{n}) = \sum_l \sum_\tau g_l^a U_l^{1\tau}(\mathbf{n}) S_l^\tau(\Omega). \qquad (4.9)$$

Here $\Omega = (\theta, \varphi)$ is the direction of observation, S_l^τ are the site-symmetry-adapted surface harmonics and $U_l^{1\tau}$ the molecular rotator functions. We take advantage of the fact that all nuclei of the C_{60} molecule are located on a single spherical shell. The orientational density distribution function is obtained by thermally averaging over the orientations $\omega(\mathbf{n})$ (Press & Hüller, 1973*a*).

In the disordered phase (Copley & Michel, 1993), where the site symmetry is A_{1g}, we get, by using (3.5) and (3.6),

$$f(\Omega) = 60/4\pi + \gamma_6^{(1)} K_6^{(1)}(\Omega) + \gamma_{10}^{(1)} K_{10}^{(1)}(\Omega) + \sum_{\rho=1}^{2} \gamma_{12}^{(\rho)} K_{12}^{(\rho)}(\Omega) + \ldots . \qquad (4.10)$$

In the ordered phase, the orientational density distribution depends on the sublattice. Performing the thermal average over the molecular orientations, we take into account relations (2.10) and (3.11) and obtain

$$f(\Omega; \sigma) = \sum_l \sum_\rho \gamma_l^{(\rho)} K^{(\rho)}(\Omega) + \sum_{i=1}^{3} g_{10}^a \eta_{10}^i(\sigma) S_{10}^i(\Omega). \qquad (4.11)$$

The first term on the right-hand side refers to the modes of A_{1g} symmetry. The second term accounts for the order parameter where we restrict ourselves to the components

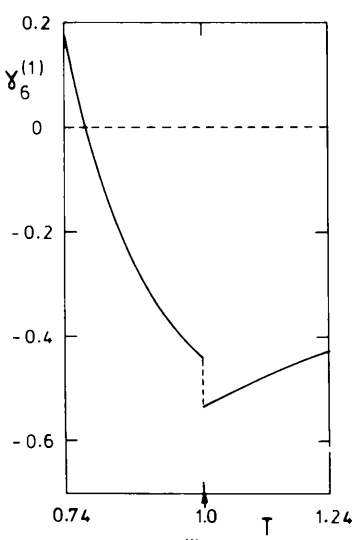

Fig. 2. Temperature evolution of $\gamma_6^{(1)}$. In the disordered phase we use expression (3.6) and in the ordered phase (3.11). The coefficients $w_l^{(\rho)}$ are taken from Table 1 and the order-parameter values from Table 3.

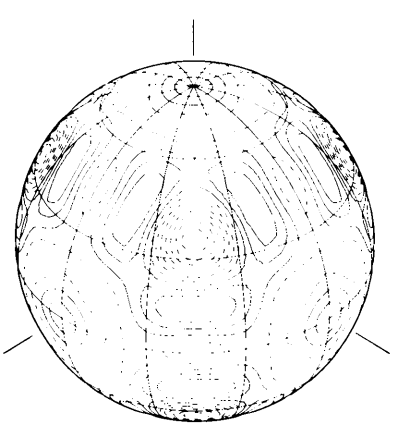

Fig. 3. Orientational density distribution function in the disordered phase ($T = 1.238T_1$), present theory. The orientational density distribution function is viewed down one of the ⟨111⟩ directions.

of symmetry T_{2g}, $\rho = 3$, belonging to the manifold $l = 10$. Formally, the A_{1g} contributions in (4.10) and (4.11) are similar; however, the coefficients $\gamma_l^{(\rho)}$ are different. In the disordered phase they are calculated with the use of the crystal field V_{CF}, but in the ordered phase with the molecular field V_{MF}. We have used the theoretical values of $\gamma_l^{(\rho)}$ from Table 3 to calculate the orientational density distribution as a function of the polar angles $(\theta, \varphi) \equiv \Omega$. In the disordered phase, we have plotted (4.10) for $f(\Omega)$. The result is shown in Fig. 3. Our theoretical result reproduces the overall important characteristics of the experiment (Chow *et al.*, 1992), namely excess scattering close to the ⟨110⟩ bonding directions and scattering deficit along ⟨111⟩.

In Fig. 4(*a*), we have drawn the orientational distribution function in the ordered phase, calculated by means of (4.11) for the sublattice (0,0,0). The coefficients $\gamma_l^{(\rho)}$ and the order-parameter amplitude are taken from Table 3 for $T = 0.941T_1$. For comparison, we show in Fig. 4(*b*) contours of maximum scattering density obtained from high-resolution neutron powder diffraction data at $T = 230$ K (*i.e.* $0.885T_1$, for $T_1 = 260$ K, experimental). The positions of maximum density derived from experiment all coincide with regions of maximum intensity of the theoretical plot. In obtaining Fig. 4(*a*), it is essential that the amplitude η_{10} is negative. The negative value of the order-parameter amplitude is a consequence of the large negative value of the crystal-field coefficient $w_{12}^{(2)}$.

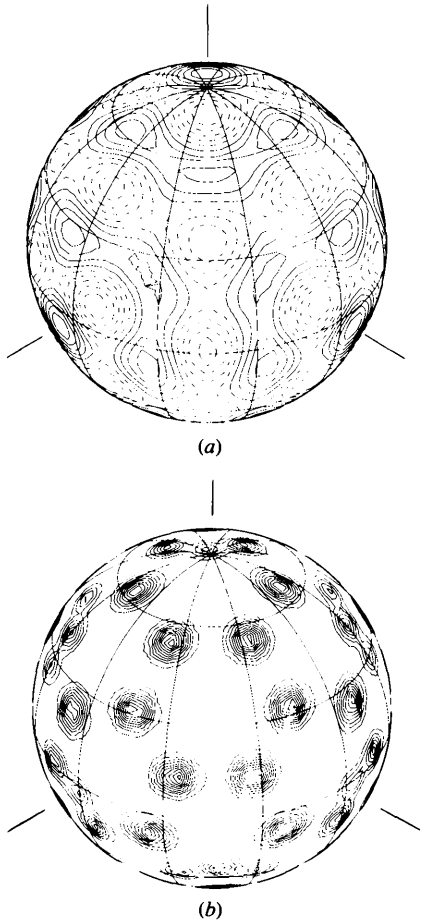

(*a*)

(*b*)

Fig. 4. (*a*) Orientational density distribution function in the ordered phase at $T = 0.941T_1$, present theory; (*b*) orientational density distribution function obtained from neutron powder diffraction data at $T = 0.885T_1$, experimental. The orientational density distribution functions are viewed down the unique three-fold [111] direction.

5. Discussion: effective potential

We have presented theoretical and experimental results on the diffraction coefficients $\gamma_l^{(\rho)}$ in the disordered and in the ordered phase. The main question we want to answer here is: how far do these results contribute to our understanding of solid C_{60}?

We first discuss the disordered phase. The coefficients $\gamma_l^{(\rho)}$ depend on the crystal-field coefficients $w_i^{(\rho)}$. The latter are related to the details of the intermolecular potential: the location of interaction centres on the C_{60} molecule (Sprik, Cheng & Klein, 1992) and the strength of the interactions (repulsive Born–Mayer, attractive van der Waals forces) between centres on different molecules. Centres with repulsive interactions on double bonds give positive contributions to $w_6^{(1)}$, $w_{12}^{(1)}$ and $w_{12}^{(2)}$ but negative contributions to $w_{10}^{(1)}$ (Copley & Michel, 1993), while atomic centres give negative contributions to all these coefficients. These subtleties render a parametrization of the intermolecular potential difficult, they also imply that in particular $w_6^{(1)}$ is very sensitive to a change of the lattice constant (Lamoen & Michel, 1994). As we have seen in the previous section, the most relevant experimental information on the crystal field has been obtained from single-crystal X-ray synchrotron diffraction experiments (Chow *et al.*, 1992). The results allow a comparison between experiment and theory. Studying the angular dependence of the crystal field V_{CF}, (2.4), by rotating the C_{60} molecule counterclockwise by an angle ψ about a [111] axis away from the standard orientation, Lamoen & Michel (1993*a*, 1994) found that the crystal field exhibits not only an absolute minimum at $\psi = 98°$ but also a secondary minimum at 38°. This secondary minimum is more sensitive to a change of the lattice constant a than the primary minimum. These minima in the single-molecule potential had been previously obtained in the disordered phase (David *et al.*, 1991; David, Ibberson, Dennis, Hare & Prassides, 1992) from the interpretation of neutron powder diffraction data at low T. At room temperature, however, the experiemental data of Chow *et al.*, (1992), as analysed in the work of Axe, Moss & Neumann (1994), did not exhibit the secondary minimum in the cystal-field potential. During the revision of the present work, we were informed by an erratum added to Axe, Moss & Neumann (1994) that a re-evaluation of the 300 K Bragg data analysis has led to slightly revised coefficients. As a

Table 5. *Effective crystal-field coefficients* $\bar{w}_l^{(\rho)}(T)$ (K) *for two different temperatures,* $T_1 = 201.9\,K$

l, ρ	$T = T_1$	$T = 0.743\,T_1$
6,1	455.22	−124.86
10,1	−195.90	−451.58
12,1	−86.36	−494.77
12,2	−591.11	−1146.39

result of these corrections, a distinct secondary minimum now appears at $\psi \simeq 38°$. The agreement between experiment and theory (Lamoen & Michel, 1994) is thereby improved. We are looking forward to a forthcoming paper by Chow *et al.* We expect that the new experimental data will be very helpful if we want to optimize the modelling of the intermolecular potential.

We now discuss the situation in the ordered phase. The main result of the previous section is the renormalization of the coefficients $\gamma_l^{(\rho)}$. The calculated temperature evolution is in qualitative agreement with the experimental data of Fig. 1, although the theoretical value of $\gamma_{10}{}^{(1)}$ is too large. The renormalization of the coefficients $\gamma_l^{(\rho)}$ can be translated in a replacement of the potential V_{CF} by an effective potential $\bar{V}_{CF}$ that depends on temperature. Indeed, from the calculated diffraction coefficients in the ordered phase, we define effective crystal-field coefficients of A_{1g} symmetry by inverting (4.1):

$$\bar{w}_l^{(\rho)}(T) = [-T(2l+1)/g_l^a]\gamma_l^{(\rho)}(T). \qquad (5.1)$$

Taking the coefficients $\gamma_l^{(\rho)}(T)$ from Table 3, we obtain for two different temperatures the values of $\bar{w}_l^{(\rho)}$ given in Table 5. The effective crystal field per molecule is given by

$$\bar{V}_{CF}(\omega) = \sum_l \sum_{\tau_{1g}} \bar{w}_l^{\tau_{1g}} U_l^{1\tau_{1g}}(\omega). \qquad (5.2)$$

Restricting ourselves to values $l \leq 12$, we have plotted in Fig. 5 the potential $\bar{V}_{CF}(\psi)$ as a function of the rotation angle ψ for two different temperatures. Notice the absolute minimum at $\psi = 98°$ and the relative minimum at 38°. With decreasing temperature, both minima get deeper; however, the change of the minimum at 38° is more pronounced. By studying the angular dependence of the function $U_6^{1\tau_{1g}}$ (see Lamoen & Michel, 1993*a*), one realizes that the temperature evolution of the potential minimum at 38° can be traced back to the change of sign of $\gamma_6^{(1)}$ or equivalently of $\bar{w}_6^{(1)}$. The decrease of $\bar{w}_6^{(1)}$ with decreasing T means that the repulsive forces between double bonds on neighbouring molecules become less efficient. This situation is reminiscent of the Virial theory of non-ideal gasses (see *e.g.* Landau & Lifschitz, 1966). There, the repulsive part of the potential is strong at high T and becomes less effective at low T. Extending the concept of molecular field potential [see equation (2.9)], we define an effective molecular field at a site on sublattice σ

$$\bar{V}_{MF}(\omega;\sigma) = \bar{V}_{CF}(\omega) - \sum_{i=1}^{3} J_{10\,10} U_{10}^i(\omega)\eta_{10}^i(\sigma), \qquad (5.3)$$

where U_{10}^i refers to the ith component of T_{2g} symmetry. In Fig. 6, we have drawn the effective molecular-field potential at site (0,0,0) as a function of the rotation angle ψ. Here again we find that the absolute minimum at 98°, while the relative minimum at 38° is becoming more pronounced with decreasing T.

The minima in the potential $V(\omega)$ correspond to maxima in the orientational probability distribution: $P(\omega) \propto \exp[-V(\omega)/T]$. The preferential orientation at $\psi = 98°$ was first identified by neutron powder diffraction at low T in the ordered phase (David *et al.*, 1991). Subsequently (David, Ibberson, Dennis, Hare & Prassides, 1992), a secondary orientation at 38° was identified by the same experimental method. The existence of these preferential orientations could be

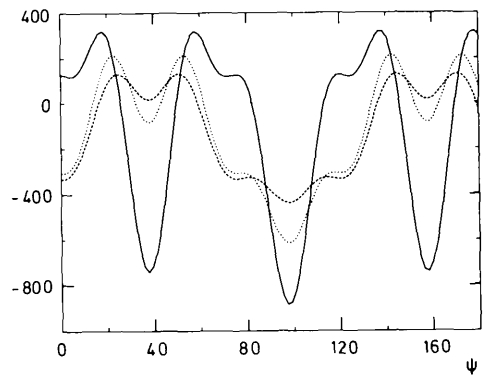

Fig. 5. Angular dependence of the crystal-field potential V_{CF} in the disordered phase (dashed line), and of the effective crystal-field potential $\bar{V}_{CF}$ at T_1 (dotted line) and at $0.743T_1$ (continuous line). Energy in K. The molecule is rotated counterclockwise around an axis [111] by an angle ψ.

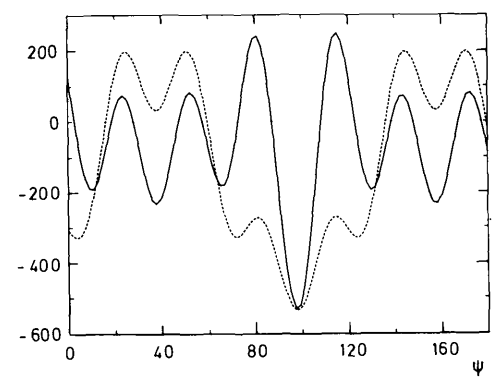

Fig. 6. Angular dependence of the effective molecular-field potential $\bar{V}_{MF}$ for $T = T_1$, $\eta_{10} = -0.067$ (dashed line) and $T = 0.743T_1$, $\eta_{10} = -0.300$ (continuous line). Energy in K.

traced back to details of the molecular structure. Double bonds fusing two hexagons on a C_{60} molecule constitute electron-rich regions. Double bonds on neighbouring molecules repell each other. In an optimized configuration, electron-rich regions of a central molecule face electron-poor regions (pentagon or hexagon faces for $\psi = 98$ and $\psi = 38°$, respectively) of neighbouring molecules. Furthermore, the occurrence of a secondary minimum at $\psi = 38°$ was related to the possible existence of an orientational glass (David *et al.*, 1992); David, Ibberson & Matsuo, 1993). Subsequently, heat-capacity measurements (Matsuo *et al.*, 1992), high-resolution dilatometry experiments (Gugenberger *et al.*, 1992), low-frequency elastic properties studies (Schranz *et al.*, 1993) and X-ray studies on single crystals (Sakaue *et al.*, 1994) have provided additional support for the orientational glass concept. At low T, more than 80% of the molecules occupy the 98° orientation in the $Pa\bar{3}$ structure, but this occupancy remains constant with decreasing $T \leq 90$ K. About 20% of the molecules remain frozen in the 38° orientation (David *et al.*, 1992). Our calculations demonstrate that the 38° minimum of the effective potential gets deeper with decreasing T, therefore it is more likely that a constant fraction of molecules remain trapped in the wrong orientation. From these considerations, we conclude that the orientational glass state here manifests itself as a single-particle freezing; however, the renormalization of the effective single-particle potential is driven by the orientational ordering, which is a collective effect.

One of the authors (KHM) acknowledges useful discussions with P. C. Chow. This work has been partly financially supported by the Science Foundation of Belgium.

References

AXE, J. D., MOSS, S. C. & NEUMANN, D. A. (1994). *Solid State Physics* 48, edited by H. E. EHRENREICH & F. SPAEPEN, pp. 149–214. New York: Academic Press.

BETHE, H. (1929). *Ann. Phys. (Leipzig)*, **3**, 133–142.

BRADLEY, C. J. & CRACKNELL, A. P. (1972). *The Mathematical Theory of Symmetry in Solids*. Oxford: Clarendon Press.

BÜRGI, H.-B., BLANC, E., SCHWARZENBACH, D., LIU, S., LU, Y.-J., KAPPES, M. M. & IBERS, J. A. (1992). *Angew. Chem. Int. Ed. Engl.* **31**, 640–642.

BÜRGI, H.-B., RESTORI, R. & SCHWARZENBACH, D. (1993). *Acta Cryst.* B**49**, 832–838.

CHOW, P. C., JIANG, X., REITER, G., WOCHNER, P., MOSS, S. C., AXE, J. D., HANSON, J. C., MCMULLAN, R. K., MENG, R. L. & CHU, C. W. (1992). *Phys. Rev. Lett.* **69**, 2943–2946.

COPLEY, J. R. D. & MICHEL, K. H. (1993). *J. Phys. Condens. Matter*, **5**, 4353–4370.

DAVID, W. I. F., IBBERSON, R. M., DENNIS, T. J. S., HARE, J. P. & PRASSIDES, K. (1992). *Europhys. Lett.* **18**, 219–225.

DAVID, W. I. F., IBBERSON, R. M. & MATSUO, T. (1993). *Proc. R. Soc. London Ser. A*, **442**, 129–146.

DAVID, W. I. F., IBBERSON, R. M., MATTHEWMAN, J. C., PRASSIDES, K., DENNIS, T. J. S., HARE, J. P., KROTO, H. W., TAYLOR, R. & WALTON, D. R. M. (1991). *Nature (London)*, **353**, 147–149.

DWORKIN, A., SZWARC, H., LEACH, S., HARE, J. P., DENNIS, T. J. S., KROTO, H. W., TAYLOR, R. & WALTON, D. R. M. (1991). *C. R. Acad Sci. Paris. Ser.* II, **213**, 979–981.

FLEMING, R. M., SIEGRIST, T., MARSH, P. M., HESSEN, B., KORTAN, A. R., MURPHY, P. W., HADDON, C., TYCKO, R., DABBAGH, G., MUJSCE, A. M., KAPLAN, M. L. & ZAHURAK, S. M. (1991). *Mater. Res. Soc. Symp. Proc.* **206**, 691–693.

GUGENBERGER, F., HEID, R., MEINGAST, C., ADELMANN, P., BRAUN, M., WÜHL, H., HALUSKA, M. & KUZMANY, H. (1992). *Phys. Rev. Lett.* **69**, 3774–3777.

HARRIS, A. B. & SACHIDANANDAM, R. (1992). *Phys. Rev. B*, **46**, 4944–4957.

HEID, R. (1993). *Phys. Rev. B*, **47**, 15912–15922.

HEINEY, P. A., FISCHER, J. E., MCGHIE, A. R., ROMANOV, W. J. DENENSTEIN, A. M., MCCAULEY, J. P. JR, SMITH, A. B. III & COX, D. E. (1991*a*). *Phys. Rev. Lett.* **66**, 2911–2914.

HEINEY, P. A., FISCHER, J. E., MCGHIE, A. R., ROMANOV, W. J. DENENSTEIN, A. M., MCCAULEY, J. P. JR, SMITH, A. B. III & COX, D. E. (1991*b*). *Phys. Rev. Lett.* **67**, 1468.

HEINEY, P. A., VAUGHAN, G. B. M., FISCHER, J. E., COUSTEL, N., COX, D. E., COPLEY J. R. D., NEUMANN, D. A., KAMITAKAHARA, W. A., CREEGAN, K. M., COX, D. M., MCCAULEY, J. B. JR & SMITH, A. B. III (1992). *Phys. Rev. B*, **45**, 4544–4547.

JAMES, H. M. & KEENAN, T. A. (1959). *J. Chem. Phys.* **31**, 12–41.

KRÄTSCHMER, W., LAMB, L. D., FOSTIROPOULOS, K. & HUFFMAN, D. R. (1990). *Nature (London)*, **347**, 354–358.

KROTO, H. W., HEATH, J. R., O'BRIEN, S. C., CURL, R. F. & SMALLEY, R. E. (1985). *Nature (London)*, **318**, 162–163.

LAMOEN, D. & MICHEL, K. H. (1993*a*). *Z. Phys.* B**92**, 323–330.

LAMOEN, D. & MICHEL, K. H. (1993*b*). *Phys. Rev. B*, **48**, 807–813.

LAMOEN, D. & MICHEL, K. H. (1994). *J. Chem. Phys.* **101**, 1435–1443.

LANDAU, L. D. & LIFSCHITZ, E. M. (1966). *Statistische Physik*, §73. Berlin: Akademie-Verlag.

LIU, S., LU, Y.-J., KAPPES, M. M. & IBERS, J. A. (1991). *Science*, **254**, 408–410.

MATSUO, T., SUGA, H., DAVID, W. I. F., IBBERSON, R. M., BERNIER, P., ZAHAB, A., FABRE, C., RASSAT, A. & DWORKIN, A. (1992). *Solid State Commun.* **83**, 711–715.

MICHEL, K. H. (1992). *Z. Phys.* B**88**, 71–78.

MICHEL, K. H., COPLEY, J. R. D. & NEUMANN, D. A. (1992). *Phys. Rev. Lett.* **68**, 2929–2932.

MICHEL, K. H. & PARLINSKI, K. (1985). *Phys. Rev. B*, 31, 1823–1835.

MORET, R., ALBOUY, P. A., AGAFANOV, V., CEOLIN, R., ANDRÉ, D., DWORKIN, A., SZWARC, H., FABRE, C., RASSAT, A., ZAHAB, A. & BERNIER, P. (1992). *J. Phys.* I (*France*), **2**, 511–515.

NEUMANN, D. A., COPLEY, J. R. D., CAPPELLETTI, R. L., KAMITAKAHARA, W. A., LINDSTROM, R. M. CREEGAN, K. M., COX, D. M., ROMANOV, W. J., COUSTEL, N., MCCAULEY, J. P. JR, MALISZEWSKY, N. C., FISCHER, J. E. & SMITH, A. B. III (1991). *Phys. Rev. Lett.* **67**, 3808–3811.

PAPOULAR, R. J., ROTH, G., HEGER, G., HALUSKA, M. & KUZMANY, H. (1993). *Electronic Properties of Fullerenes. Springer Series in Solid-State Sciences*, No. 117, edited by H. KUZMANY, J. FINK, M. MEHRING & S. ROTH, pp. 195–199. Berlin: Springer.

PICK, R. M. & YVINEC, M. (1980). *J. Phys. (Paris)*, **41**, 1053–1059.

PRESS, W. & HÜLLER, A. (1973*a*). *Acta Cryst.* A**29**, 252–256.

PRESS, W. & HÜLLER, A. (1973*b*). *Phys. Rev. Lett.* **30**, 1207–1211.

RAPCEWICZ, K. & PRZYSTAWA, J. (1994). *Phys. Rev B*, **49**, 13193–13196.

SACHIDANANDAM, R. & HARRIS, A. B. (1991). *Phys. Rev. Lett.* **67**, 1467.

SAKAUE, K., TOYODA, N., KASATANI, H., TERAUCHI, H., ARAI, T., MURAKAMI, Y. & SUEMATSU, H. (1994). *J. Phys. Soc. Jpn Lett.* **63**, 1237–1240.

SCHRANZ, W., FUITH, A., DOLINAR, P., WARHANEK, H., HALUSKA, M. & KUZMANY, H. (1993). *Phys. Rev. Lett.* **71**, 1561–1564.

SPRIK, M., CHENG, A. & KLEIN, M. L. (1992). *J. Phys. Chem.* **96**, 2027–2032.

YILDIRIM, T., HARRIS, A. B., ERWIN, S. C. & PEDERSON, M. R. (1993). *Phys. Rev. B*, **48**, 1888–1895.

YVINEC, M. & PICK, R. M. (1980). *J. Phys. (Paris)*, **41**, 1045–1052.